IS&T/OSA

Optics & Imaging in the Information Age

October 20 – 24, 1996
Rochester, New York

Co-Sponsored by The Optical Society of America and The Society for Imaging Science and Technology

Published by IS&T—The Society for Imaging Science and Technology
7003 Kilworth Lane, Springfield, Virginia 22151 USA
Phone (703) 642-9090; Fax (703) 642-9094; e-mail info@imaging.org

Three Dimensional Momentum Distributions of Recoil-Ions and Photoelectrons

J. Ullrich, R. Dörner†, O. Jagutzki†, V. Mergel†, R. Moshammer†, H. Schmidt-Böcking†, L. Spielberger†, M. Unverzagt† and T. Vogt†*

** GSI, Gesellschaft für Schwerionenforschung mbH, Darmstadt, Germany*

† Institute für Kernphysik, Universität Frankfurt, Frankfurt, Germany

Abstract

A novel high-resolution technique, the Multi-Electron-Recoil-Ion Momentum Spectroscopy, allows to determine in coincidence the three dimensional momentum vectors of the ion and up to three electrons created in any photo ionization event. At a solid angle of 4 π the energy-resolutions for ions and electrons are ±2μeV and ±10meV, respectively.

Introduction

Experimentally, photoionization of atoms can be investigated by observing the reaction products, namely electrons, ions, fluorescence light or the attenuation of the incident light. Traditionally, electrons have been analyzed differential in their emission angle and energy using electrostatic, magnetic, or time-of-flight methods (for a review see V. Schmidt[1]). Depending on the resolution to be obtained typical detection solid angles $\Delta\Omega_e$ of not more than $\Delta\Omega_e \approx 10\text{-}3$ of 4π are achieved. Thus, the coincident detection of two electrons, most important to investigate electron-electron correlation in photon induced multiple ionization reactions is already an extremely difficult task and only few so-called (γ,2e) investigations have been reported[2-6] with coincidence rates in the mHz to Hz regime. Recently, an efficient electron-imaging detector ($\Delta\Omega e \approx 4\pi$) has been developed[7] to investigate multiphoton ionization of target atoms in intense laser fields. Here photoelectrons are projected onto a phosphor screen by a dc electric field and their spatial image is recorded using a video camera. This technique delivers a projection of the three-dimensional one-electron momentum space onto two dimensions. In numerous experiments photoions have been analyzed with respect to their charge to mass ratio q/m partly in coincidence with the emitted photo-electron using magnetic mass analyzers, quadrupole mass filters or efficient, large-solid angle time-of-flight methods.[1]

In this contribution we report on imaging techniques that determine the charge state and, in addition, the complete final state momentum vector of the recoiling photoion $\mathbf{P}_R$, the so-called "Recoil-Ion Momentum Spectroscopy" (RIMS) or "Cold Target Recoil-Ion Momentum Spectroscopy" (COLTRIMS).[8] Applying well controlled electric fields, ions emerging from a cold target jet ($T \leq 50$mK) are efficiently projected ($\Delta\Omega_e \approx 4\pi$) onto large area position sensitive detectors. Their initial momentum is calculated from the hitting position on the detector and their time-of-flight with extreme precision corresponding to an energy resolution of a few μeV. Originally, RIMS has been developed to investigate ion-atom collisions but recently has been exploited to obtain detailed information on He double ionization by photon impact at incident photon energies between 80 eV and 58 keV. This is the entire energy range available at modern synchrotron radiation facilities. Mapping the complete momentum vector of the recoiling target ion after photoionization at high γ-energies for the first time allowed to separate contributions from Compton scattering and photo absorption to helium double ionization[9,10] (Compton scattering contributions to He single ionization by a similar, but low-resolution technique has been reported by Samson et al.[11]). At low and medium incident photon energies the complete control of the kinematics enabled unprecedented accurate measurements of total cross section ratios by integrating over all recoil-ion momenta.[12]

Novel highly efficient imaging techniques for electrons have been developed at GSI and combined with high-resolution RIMS.[13-15] In these "reaction microscopes" electrons with energies below 1 keV can be projected by combinations of electric and magnetic fields onto multi-hit capable detectors reaching a solid angle of more than 50% of 4π. Using nanosecond position readout methods and advanced multi-hit electronics the arrival time and position of up to 16 electrons emerging from a single multiple ionization event can be recorded. For single ionization of He induced by the virtual photon field of fast heavy ions Moshammer et al.[16,17] succeeded in visualizing the entire 9-dimensional final-state momentum space. More recently we have performed kinematically complete experiments on helium double[18] and neon triple ionization by ion-induced intense pulses of virtual photons. Helium double photoionization by monochromatic 80 eV photons was explored[19] using similar devices mapping the entire mod-squared wave function of the final three particle state i.e. for all possibilities in momentum sharing within the three particle continuum.

Experimental Technique

In this part the most advanced (Multi-)Electron - Recoil-Ion Momentum Spectrometers ("reaction microscopes") are briefly described. More detailed technical information on such spectrometers have been given by Moshammer et al,[14] Dörner et al[20] and Kollmus et al.[15] Former concepts, the development of such spectrometers as well as their ap-

plication in ion-atom collisions have been shortly summarized by Ullrich et al.[8] and will be discussed in detail in an upcoming an review on the field.[21]

General Concept

(Multi-)Electron - Recoil-Ion Momentum Spectrometers are based on well localized inherently cold atomic (molecular) targets ensuring a "perfect" preparation of the initial target momentum. Providing a cold target is essential for the recoil-ion momentum resolution since the momenta to be measured are often on the order of or even below the typical thermal momenta of atoms at room temperature. Cooling is realized by supersonic expansion forming a cold atomic (molecular) beam which is crossed by the photon (or any other projectile) beam in the presence of well defined electric (Figure 1) and, in most advanced designs, electric plus magnetic fields (Figure 2). This way, ions and electrons (or ionic fragments of molecules) created during the collision are efficiently guided onto position sensitive detectors and large detection solid angles are achieved. From the final positions and their times of flight (TOF) in the apparatus the trajectories of ions and electrons are reconstructed and their initial momenta are calculated.

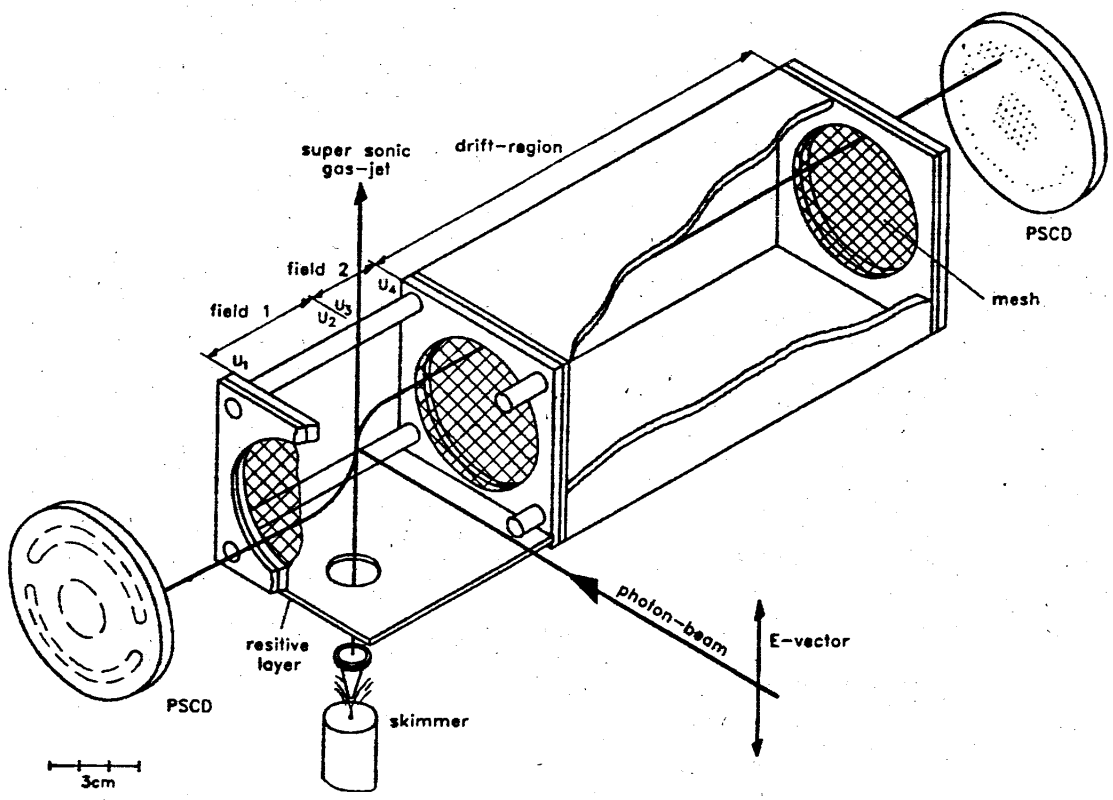

Figure 1. Electron - Recoil-Ion Momentum Spectrometer with two position sensitive channel plate detectors (PSCD).

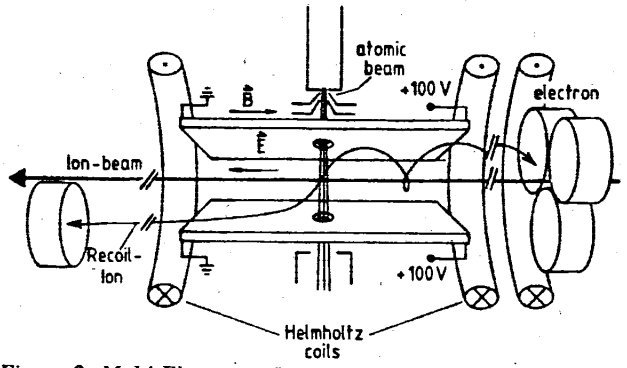

Figure 2. Multi-Electron - Recoil-Ion Momentum Spectrometer with combined electric and magnetic projection fields for the electrons.

Supersonic Expansion

Localized atomic or molecular targets are generated exploiting the features of adiabatic supersonic expansion of the target gas.[14,22] Under ideal conditions the total entropy H of a thermodynamical system which is $5/2 \cdot k \cdot T_0$ (k: Boltzmann constant, T_0: temperature) for an ideal gas, can be converted into directed kinetic energy by quasistatic adiabatic expansion: the atoms move with a momentum along the expansion of $P_{jet} = (5 \cdot k \cdot T_0 \cdot M_R)^{1/2}$ which is about 5.9 a.u. (atomic unit) for helium at 300 K (E_{jet} = 64 meV) and 1.9 a.u. at 30 K. In praxi this is not achieved. The actual quality of the jet is expressed by its speed ratio $S = (5T_0/2T)^{1/2}$ where T is the left-over internal jet temperature after the expansion approaching zero in the ideal case. In the various spectrometers the gas is pressed through a thin nozzle (typical diameters 5μm to 50μm) at pressures before the expansion between 0.2 and 30 bar and temperatures of the gas reservoir between 14 K and 300 K. The quality of the

jet, its inherent temperature, strongly depends on the expansion parameters and different values might be ideal for different experimental situations. The optimum momentum resolution is achieved by precooling the gas simultaneously using high pressures before the expansion. Depending on the gas to be used the ultimate limit is reached if the gas starts to form dimers, trimers or clusters during expansion (various groups plan to investigate reactions with cluster targets in the near future). The expanding gas then is skimmed in one, two or even 4 stages[23] in order to form a well defined atomic beam and to guarantee good vacuum conditions in the interaction chamber.

For example, the COLTRIMS set-up developed by Mergel et al.,[24] providing the presently best momentum resolution, is shown in Figure 1. Here, the rare gas (He, Ne, Ar, etc.) is precooled to a temperature of approximately 15 K (for He) at a pressure between 200 and 1000 mbar using a cryogenic cold head. The gas then expands through a 30 μm hole forming a supersonic jet. The inner jet fraction passes through a 0.3 mm skimmer into the scattering chamber yielding an atomic beam with a diameter of about 1 mm at the intersection point with the projectile beam. The internal momentum spread of the target in the direction of the gas jet is determined by the parameters of the expansion and is typically below ±0.05 a.u. In the direction transverse to the jet expansion an even smaller momentum spread between ±0.05 a.u. In the direction transverse to the jet expansion an even smaller momentum spread between ±0.015 a.u. and ±0.035 a.u. is achieved by skimming of the atomic beam. The momentum resolutions finally obtained in the two directions perpendicular to the incident photon beam depend on the size of the overlap volume of the photon and atomic beam (for details see Moshammer et al.[14]). Values in the order of $\pm 10^{-3}$ a.u. can be anticipated using brilliant photon beams from 3rd generation light sources with beam diameters as small as 50 μm.

Extraction of the Recoil Ions

The atomic beam is intersected with a photon (projectile) beam and target ions are produced in ionizing atomic reactions. Depending on the actual investigated, an appropriate electrostatic field is applied at the interaction region (see Figure 1) such that all recoil-ions with the momenta of interest are projected onto the surface of a two-dimensional position sensitive (2DPS) multi-channel plate (MCP) detector. In the apparatus shown in Figure 1 a 10 m long 7μm carbon fiber is wound around four supporting germanium coated isolator screws homogeneously dividing the extraction voltage to ground potential according to the electric resistance of the fiber. Recently, non homogeneous, lens-like extraction fields E_{ex} have been developed which guide ions having identical initial momenta but different starting positions in the overlap volume of the gas jet with the photon beam to the same position on the MCP detector.[24] Consequently, the momentum resolution in the two dimensions perpendicular to the extraction is no longer restricted (to first order) by the uncertainty of the starting positions. In all spectrometers a drift region follows the extraction field (see Figure 1). Its length is adapted to the length and form of E_{ex} such that the ions created at different positions within the overlap region also focus in time of flight on the detector to first order. Thus, RIM-spectrometers which focus in all three spatial dimensions have become feasible and the momentum uncertainty due to the finite size of the source volume becomes negligibly small.

Another set-up has been used to investigate photo dissociation of atoms in the virtual photon field of relativistic heavy ions at GSI.[13-15] Here recoil-ions are likewise extracted into the longitudinal direction (along the projectile beam) generating the extraction field between to ceramic plates (see Figure 2). The plates are covered by two burned in resistive layers with different resistances in such a way that any direction of the electric field vector can be generated (in the transverse or longitudinal or any other direction). Voltages can be applied such that position-focusing electric fields are generated for the transverse momentum components. The longitudinal momentum component is time-focused. This concept is extremely versatile which turned out to be essential for the combination of a RIM spectrometer with the novel magnetic electron analyzers. The dimensions of this spectrometer are about twice as large as in other set ups resulting in a factor of 30 increased dynamic range in the direction of extraction (recoil ion longitudinal momenta of up to $P_{R\|} \leq 150$ a.u. are accepted) at very good momentum resolution in all directions of $\Delta P_R \leq \pm 0.08$ a.u.

Coincidences with Emitted Electrons: "Reaction Microscopes"

The invention of an extremely efficient and precise new method for the detection of electrons with energies $E_e < 1$ keV and its successful implementation into high-resolution RIM spectrometers[13-15] has lead to a decisive extension of the applicability and future potential of RIMS. These Multi-Electron - Recoil-Ion Momentum Spectrometers, which have been developed at GSI open completely new windows to explore atomic many particle reactions.

In the most recent set-up (Figure 2) longitudinal extraction of the recoil-ions in the backward direction is applied with a total extraction voltage of up to +100 V. Thus, all electrons with longitudinal backwards energies of $E_{e\|} \leq 50$ eV (potential a the point of interaction: +50 V) are accelerated downstream hitting onto three 2DPS micro channel plates. The detectors are placed in the forward direction in time-focusing geometry at a total flight path of 33 cm (same principle as described above for the ions). Applying solenoidal magnetic fields of up to 100 Gauss with its axis about along the beam axis all electrons with non-zero transverse energies $E_{e^\wedge}$ are forced onto spiral trajectories and projected on the detector with a 2π solid angle for $E_{e^\wedge} \leq 1$ keV. The electron longitudinal momenta are obtained from the TOF measured in a coincidence between each of the electrons, the projectile (photon pulse) and the recoil ion. The electron positions contain the information on their transverse momenta and azimuthal emission angles. The electron detector is equipped with a delay-line readout[25] for the fast (total delay in one direction 36 ns) position readout. All five signals from the delay-line are amplified in fast differential amplifiers, separated from noise in 300 MHz "Constant Fraction Discriminators" and finally feed into a

32 channel multi-hit "Time-to-Amplitude Converter" (TDC). Each of the channel of the TDC can accept up to 16 hits with a minimum time between two subsequent hits of less than 10 ns. Thus, in principle the complete momentum vector of up to 16 electrons can be determined simultaneously. In recent experiments on the dissociation of neon in the intense virtual photon field of fast N^{24+} projectiles the complete momentum vector of up the three emitted electrons have been measured in coincidence with the recoil-ion. The magnetic field was set such that a solid angle of 4π was reached for all electrons with $E_e \leq 50$ eV. The electron energy resolution is dependent on the momentum acceptance of the spectrometer. In most recent experiments a resolution of about $\Delta E_e = \pm 10$ meV has been reached (corresponding to a momentum resolution of $\Delta P_e = \pm 3 \cdot 10^{-2}$ a.u.) at a solid angle of 100 % of 4π for electrons with $E_e \leq 9$ eV.

It has been emphasized by Kollmus et al.[12] that unprecedented, exciting values for the electron momentum resolution are achievable in such spectrometers for low energy electrons. Due to the smaller mass of the electrons their initial state momentum uncertainty resulting from the internal temperature of the supersonic jet is only $7 \cdot 10^{-6}$ a.u. ($\Delta E_e = 6 \cdot 10^{-10}$ eV). Focusing geometries and extraction fields can be used to minimize the uncertainty due to the finite source volume and realistic resolutions as small as 10^{-4} a.u. or energy resolutions below 1 μeV may be envisaged.

Another concept, well adapted to detect very low-energy electrons ($E_e \leq 10$ eV) in combination with high-resolution RIMS was used by Dörner et. al.[15,21] placing a position sensitive detector for the emitted electrons in the direct vicinity of the interaction volume opposite to the recoil-ion detector (see Figure 1). Without a magnetic field a 4π detection solid angle has only achieved for electrons with momenta transverse to the extraction field below 0.9 a.u. Performing a recoil-ion - electron - pulse coincidence in recent experiments on double photo ionization all three electron momentum components have been determined with this spectrometer.[21]

Kinematics of Photoionization

Absorption of a Photon

If a photon is absorbed by an atom its energy E_γ is deposited into the electron shell and, for single photo ionization, one electron emerges with an energy of $E_e = E_\gamma - E^{bind} - E^{exc}$ having a momentum of $P_e = \sqrt{2E_e}$ where E^{bind} is the binding energy of the emitted electron and E^{exc} the total excitation energy of all electrons left on the target (throughout this paper atomic unit are used where the electron mass me, the electron charge e and the Planck constant $\hbar$ is equal unity ($m_e = e = \hbar = 1$)). The energy of the remaining ion E_R is negligibly small due to its large mass $E_R/E_e = \mu$ with μ being the reduced mass of the electron and the ion. The final electron momentum is compensated by the recoiling target ion resulting in P_R-distributions on spheres in momentum space with radii $P_R = P_e$ in the center of mass system depending on the incident photon energy and the excitation energy of the remaining target electrons. In the laboratory system the sphere for the ion is shifted along the photon beam direction by $P_{R\|} = P_\gamma = E_\gamma/c$ (the momentum of the incoming photon is mainly transferred to the ion and the electron momentum sphere is only shifted by $P_{e\|} = \mu \cdot P_\gamma$). The intensity distribution on these spheres mirror the angular emission characteristics of the emitted photo electron.

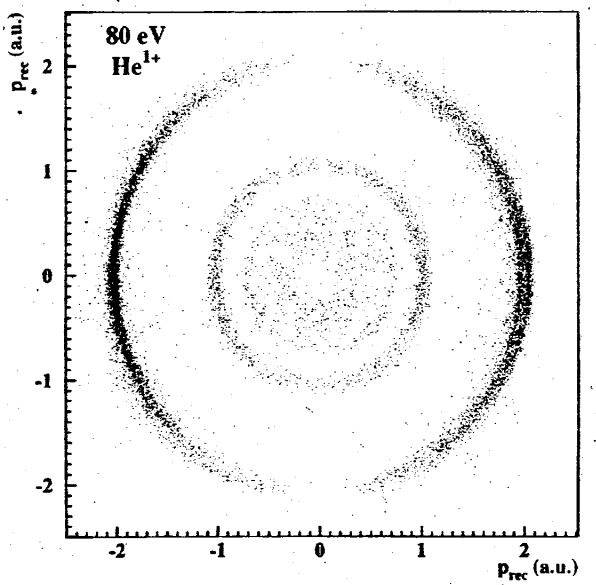

Figure 3. Momentum distribution of He1+ ions created by 100 eV linear polarized photons. The polarization axis and the electric extraction field for the ion detection is along the x-direction. The data are integrated over a momentum range of ±0.1 a.u. in the z-direction (the direction of the photon propagation).

In Figure 3 the two dimensional transverse momentum distribution of recoiling He^{1+} ions is shown for an incident photon energy of $E_\gamma = 100$ eV integrated over $P_{R\|} \leq \pm 0.1$ a.u. (note: the whole mementum sphere is measured simultaneously and only an illustrative subset is shown in Figure 3). The longitudinal shift due to the photon momentum of $P_\gamma = 0.027$ a.u. is negligibly small. The two kinematical rings observed are due to different final states of the remaining He^{1+} (outer ring: ground state, second fing: first excited state). Since linearly polarized light (along the x-axis) has been used in this experiment the intensity distribtution on the outer ring is given by the dipole emission characteristics of the emerging photo electron (ion). If the second electron is left in an exicted state (via ionization plus excitation or double excitation in the vicinity of a resonance followed by an Auger decay) the emitted electron (recoiling target ion) must not display dipole-characteristics which can and has been efficiently explored using RIMS.

Compton Scattering of a Photon

For Compton scattering of the photon dominating the photo ionization cross section at large E_γ the recoil-ion kinematics is very different from the one for photo absorption. Whereas only a bound electron can absorb a photon (the target nucleus has to compensate the emitted electron momentum) the scattering of a photon can occur on free electrons (Compton scattering) where energy and momentum conservation is fulfilled by the photon and the electron

alone ($\mathbf{P}_e = \mathbf{P}_\gamma - \mathbf{P}_{\gamma'} \times$ and $E_e = E_\gamma - E_{\gamma'} \times$ for an electron initially at rest in the laboratory system). If the electron is initially in a bound state the two-body momentum balance is modified due to the electrons initial momentum distribution in the atom ($\mathbf{P}^{in}_e$), its "Compton profile" : $\mathbf{P}_e = \mathbf{P}_\gamma - \mathbf{P}_{\gamma'} + \mathbf{P}^{in}_e$. From momentum conservation one obtains for single ionization after Compton scattering:

$$\mathbf{P}_\gamma + \mathbf{P}_{Hc} = \mathbf{P}_{\gamma'} + \mathbf{P}_R + \mathbf{P}_e$$

$$\text{or: } \mathbf{P}_R = -\mathbf{P}^{in}_e$$

in the approximation that no momentum exchange with the target nucleus occurs in the exit channel and that the initial momentum of the helium atom $\mathbf{P}_{Hc} \approx 0$ (both approximations are usually well fulfilled). Then, for ionization as a result of Compton scattering the target-ion recoil momentum is a broad distribution even for monoenergetic photon impact and mirrors the electron initial state momentum distribution.

In Figure 4 the He^{1+} recoil-ion momentum distribution in two is shown for single ionization of He by 8.8 keV photons. In addition to the kinematical sphere for photo-absorption with a radius of about 30 a.u. a narrow recoil-ion momentum distribution is observed centered around $\mathbf{P}_R = 0$ a.u. with a width of the distribution of about 1 a.u. resulting from Compton scattering of the photons. This way, the contributions of both processes to helium single and double ionization have been separated in recent experiments by Spielberger et al.[9,10]

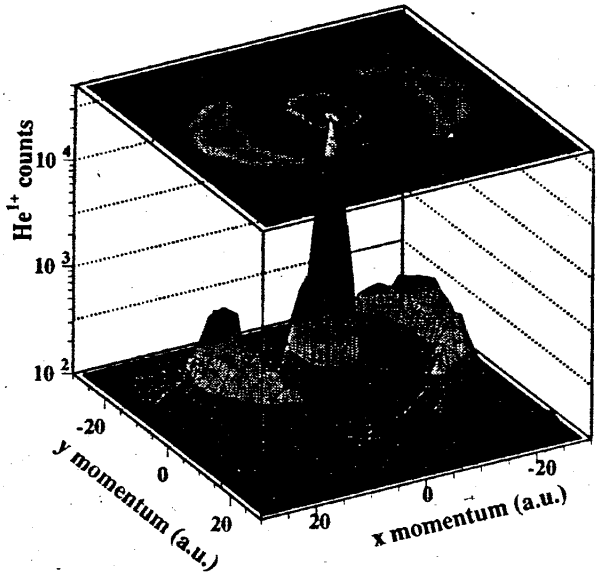

Figure 4. Momentum distribution of He1+ ions created by 8.8 keV linear polarized photons The geometry is according to Fig.3.

Selected Results

Imaging of the Complete Final State in (γ,2e) Experiments

Using a reaction microscope as shown in Figure 1 we have performed kinematically complete (γ,2e) experiments at 1eV to 80 eV above threshold[19] to explore the three-body break up of a bound system which is one of the most fundamental and still intriguing problems of atomic collision physics.[26,27] The vector momenta of all three escaping particles were determined simultaneously thus sampling the entire 9-dimensional final momentum space. At an excess energy of 1 eV above threshold a 4π solid angle was reached for all possible relative momentum partitions between the emerging two electrons and the He^{2+} ion. This is substantially different from previous experiments applying electron-electron coincidence techniques,[2-6] where only subsets have been measured in coplanar geometry (the momentum vectors of the two electrons $\mathbf{k}_1$, $\mathbf{k}_2$ are in one plane). The effective data collection efficiency with the recoil-ion technique was orders of magnitude higher than those reached in the latter experiments.

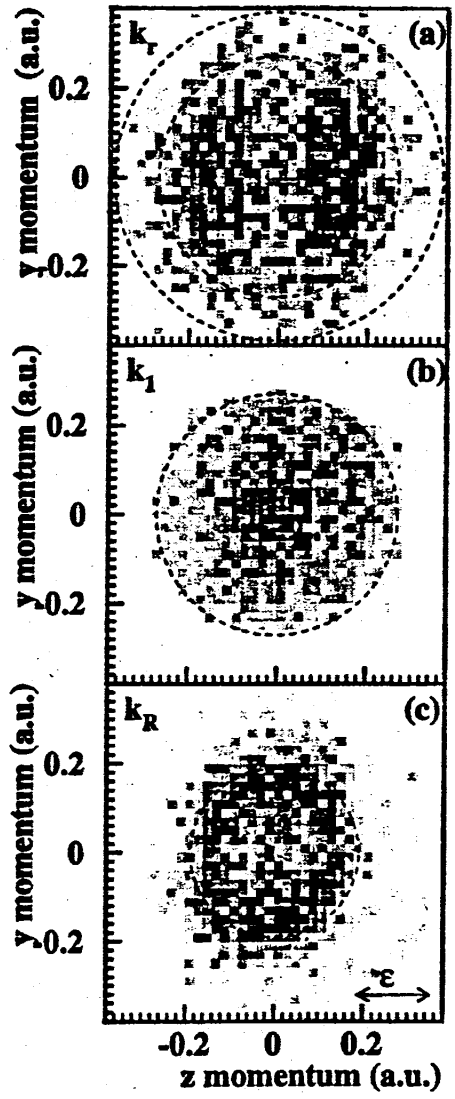

Figure 5. Momentum distribution after He double ionization 1 eV above threshold19. The z axis is the direction of the polarization vector, the data are integrated over ±0.1 a.u. in the x-direction. (a) shows the momentum distribution of the recoil-ion kr, (b) of the electron k1 and (c) of kR.

To elucidate the mechanisms of the three-body break-up 1 eV above the double ionization threshold Jacobian

momentum coordinates were chosen, i.e. $\mathbf{k}_r = \mathbf{k}_1 + \mathbf{k}_2$ and $\mathbf{k}_R = 1/2\,(\mathbf{k}_1 - \mathbf{k}_2)$ which are the electron center of mass motion and the electron-pair motion, respectively. Neglecting the incoming photon momentum the experimentally observed recoil-ion momentum $\mathbf{P}_R$ is equal to $-\mathbf{k}_r$ and the electric dipole operator is $\varepsilon \cdot r$. In Figure 5 the momentum distributions for $\mathbf{k}_r$ (the motion of the recoil-ion), $\mathbf{k}_1$ (the motion of either electron) and for $\mathbf{k}_R$ (the relative motion of the two electrons) are projected onto the y-z plane for -0.1 a.u. $< k_x <$ +0.1 a.u. where z is along the photon polarization vector and y is perpendicular to ε and to the direction of the incoming photon propagation along x. The He^{2+} recoil-ion distribution qualitatively displays a dipole distribution (Figure 5a) whereas such a behavior is found to be completely washed out in the momentum distribution of either electron (Figure 5b) due to the strong interaction of both electrons in the final state. The relative motion of the two electrons (Figure 5c), however, shows a distinct pattern indicating that the pair preferentially separates perpendicular to the photon polarization axis and, thus, to the recoil-ion motion.

The "Attosecond Microscope": Imaging the Complete Final State After Target Multiple Ionization in the Attosecond, Exawatt Virtual Photon Field of Fast Heavy Ions

Using the reaction microscope as illustrated in Figure 2, we were able to visualize the complete final state momentum distribution for helium and neon multiple ionization (up to 12 momentum components are determined in the experiment) in the intense virtual photon field produced by fast, highly-charged heavy ions. The electromagnetic field E(t,b) created at the target by the projectile depends on the relevant collision-time t and the impact parameter b of the collision. The Fourier transform of that field $E(\omega,b)$ contains a broad band of frequencies. If fast ions are used, the active time is very short and typically in the range of attoseconds (10^{-18} sec). For relativistic projectiles this time becomes even smaller due to the contraction of the field in the direction of the projectile propagation (Lienard-Wiechert potential). It is a well known technique to quantize such a field (Weizäcker-Williams method[28]) yielding a short, intense and broadband pulse of virtual photons. For 0.3 GeV Se^{28+} projectiles used in the present experiment and typical impact parameters leading to single up to triple ionization of the target the pulse time is on the order of a few attoseconds, the pulse power is in the exawatt range (10^{18} W/cm^2) and the usable bandwidth extends to several hundred electronvolts. There are no other light sources available delivering such fields being a unique tool to photo dissociate atoms, molecules, clusters or even nuclei.

In this contribution only one illustrative projection of the nine-dimensional final momentum probability distribution (mod-squared of the final state wave function) can be shown for helium double ionization by 0.3 GeV Se^{28+} impact. In Figure 6 the longitudinal (along the ion-beam direction) momentum distributions of the two emerging electrons are shown for different impact parameter regimes i.e., transverse momentum transfers to the target $P_{r\perp}$. Two features can be seen: First, there is a pattern in the data such that if one electron is fast the other one tends to be slow. It has been demonstrated before, that this pattern strongly depends on the correlation between the two electrons in the initial and final state as well as during the collision.[17,18] Second, if the impact parameter is decreased, i.e., for larger transverse momenta of the recoiling target ion higher equivalent photon energies are present in the virtual photon field. This leads to increased energies (longitudinal momenta in Figure 6) of the emitted electrons and the pattern becomes even more pronounced.

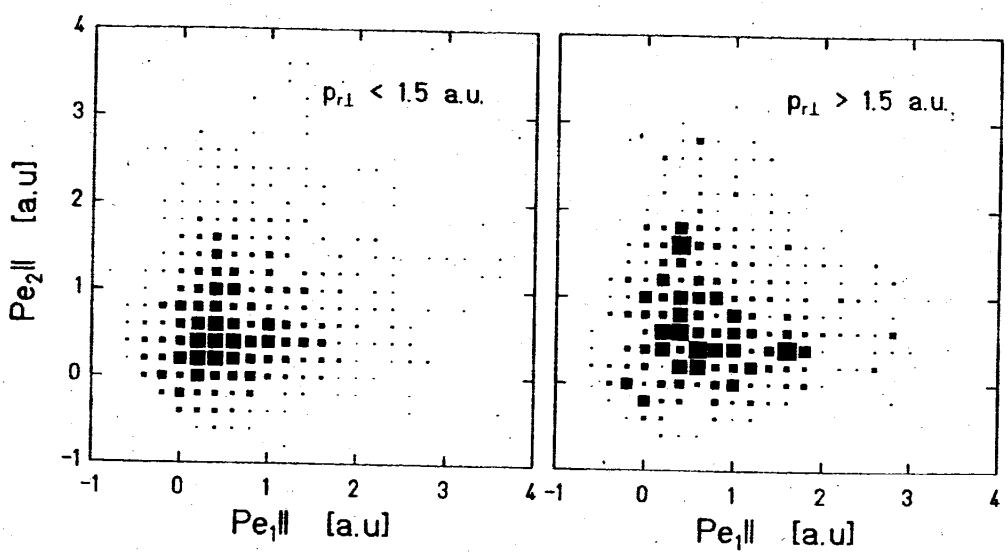

Figure 6. Longitudinal momentum (along the ion beam direction) of one electron $P_{e1\|}$ versus the one of the second electron $P_{e1\|}$ for He double ionization under the condition of large ($P_{r\perp} > 1.5$ a.u.) and small ($P_{r\perp} < 1.5$ a.u.) transverse momenta of the He^{2+} recoil ion.

Conclusions

In conclusion, applying novel imaging techniques for the recoiling target "photoion" and the photo-electrons it has been possible to map the complete final state momentum probabilities for up to three continuum electrons after photo disintegration of atoms. Such experiments have provided the most precise data on the ratio of double to single ionization cross sections for helium and, in addition, enabled the first separate measurement of this ratio for photo absorption and Compton scattering at high photon energies. These data serve as benchmarks for recent theories. Moreover, a first set of kinematically complete experiments on helium double ionization have been performed delivering experimental information with unprecedented completeness on the entire 9-dimensional momentum space for the three-body Coulomb break-up of helium. Very recently, the four-body break-up of Ne was explored in a kinematically complete experiment using the virtual photon field of fast highly-charged ions at GSI to photo disintegrate the Ne atom.

Experiments are under preparation at the Advanced Light Source (ALS) of the Lawrence Berkely Laboratory (LBL) to investigate photoionization of helium and neon further above threshold. At keV photon energies complete (γ,2eγ') experiments i.e double ionization of a target after Compton scattering of the photon are scheduled to be performed at the European Synchrotron Radiation Facility (ESRF) in Grenoble as well as at the Advanced Photon Source (APS) at the Argonne National Laboratory. Using our high-resolution multi-electron spectrometer unique experiments should become feasible to investigate the correlated emission of electrons from solids (conductors, semiconductors, super conductors etc.) after photon impact. It should be kept in mind that the momentum resolving power of our multi-electron spectrometer is on the order of $\Delta p_e/p_e \approx 10^{-3}$ when used at a third generation light source with beam spots as small as 50 μm × 50 μm. For a dynamical range of $E_e \leq 2$ eV above (multiple) ionization thresholds the absolute energy resolution for photoelectrons is below 10 meV and thus is comparable with the best spectral resolutions obtained at 3rd generation synchrotrons for photons in the energy range between 60 and 80 eV.

It has been demonstrated before, that reaction microscopes are able to image the entire momentum space of the ionic fragments after disintegration of molecules in the virtual photon field. Presently, technologies are being developed to detect the ionic fragments and, in addition, the emitted electrons after photo dissociation of simple molecules. Finally neighboring fields may take advantage of our methods for example multi-photon ionization of atoms and molecules in intense laser fields.

References

1. V. Schmidt, *Rep. Prog. Phys.* **55**, 1843, (1992).
2. O. Schwarzkopf et al. *Phys. Rev. Lett.* **70**, 3008 (1993).
3. O. Schwarzkopf et al. *J. Phys.* **B 27**, L347 (1994); **B 28**, 2847 (1995).
4. A. Huetz et al., *J. Phys.* **B 27**, L13 (1994).
5. P. Lablanquie et al., *Phys. Rev. Lett.* **74**, 2192 (1995).
6. G. Dawber et al., *J. Phys.* **B 28**, L271 (1995).
7. H. Helm et al., *Phys. Rev. Lett.* **70**, 3221 (1993).
8. J. Ullrich et al., *Comments At. Mol. Phys.* **30**, 285 (1994).
9. L. Spielberger et al., *Phys. Rev. Lett.* **76**, 4685 (1996).
10. L. Spielberger et al., *Phys. Rev. Lett.* **74**, 4615 (1995).
11. J. Samson et al., *Phys. Rev. Lett.* **72**, 3329 (1994).
12. R. Dörner et al., *Phys. Rev. Lett.* **76**, 2654 (1996).
13. J. Ullrich et al., *Nucl. Inst. Meth.* **B 98**, 375, (1995).
14. R. Moshammer et al., *Nucl. Inst. Meth.***B 108**, 425, (1996).
15. H. Kollmus et al., *Nucl. Inst. Meth.* (accepted for publication).
16. R. Moshammer et al., *Phys. Rev. Lett.* **73**, 3371 (1994).
17. R. Moshammer et al., invited contribution to *"X-96"*, Hamburg (1996).
18. R. Moshammer et al., *Phys. Rev. Lett.* **77**, 1242 (1996).
19. R. Dörner et al., *Phys. Rev. Lett.* **77**, 1024 (1996).
20. R. Dörner et al., *Nucl. Inst. Meth.* (accepted for publication).
21. J. Ullrich et al., *J. Phys.* **B**, topical review (in preparation).
22. H. Buchenau et al., *Chem. Phys.* **92**, 6875 (1990).
23. H. T. Schmidt et al., contribution to *"2nd Euroconf. on Storage Rings"*, Stockholm (1996).
24. V. Mergel, *PhD Thesis*, Universit%ot Frankfurt (1996).
25. E. Stanley et al., *IEEE Transaction ion Nuclear Science*, Vol. **35** No. 1, 348 (1998).
26. F. Maulbetsch and J.S. Briggs, *J. Phys.* **B 28**, 551 (1995).
27. J. M Feagin, *J. Phys.* **B 28**, 1495 (1995).
28. E.J. Williams, *Phys. Rev.* **45**, 729 (1934).